available at www.sciencedirect.com

ScienceDirect

journal homepage: www.elsevier.com/locate/biochempharm

# Properties of flavonoids influencing the binding to bilitranslocase investigated by neural network modelling

*Anna Karawajczyk* [a,b], *Viktor Drgan* [a,c], *Nevenka Medic* [d,1], *Ganiyu Oboh* [d,e,f], *Sabina Passamonti* [d,*], *Marjana Novič* [a,**]

[a] *National Institute of Chemistry, Hajdrihova 19, 1001 Ljubljana, Slovenia*
[b] *Leiden Institute of Chemistry, Gorlaeus Laboratoria, 2300 RA Leiden, The Netherlands*
[c] *Faculty of Chemistry and Chemical Technology, University of Ljubljana, 1001 Ljubljana, Slovenia*
[d] *Department of Biochemistry, Biophysics and Macromolecular Chemistry, University of Trieste, 34127 Trieste, Italy*
[e] *International Centre for Theoretical Physics, 34124 Trieste, Italy*
[f] *Biochemistry Department, Federal University of Technology, P.M.B. 704 Akure, Ondo State, Nigeria*

ARTICLE INFO

*Article history:*
Received 27 July 2006
Accepted 25 September 2006

*Keywords:*
Flavonoids
Bilitranslocase
Transport
Liver
QSAR modelling
Counter propagation-artificial neural network

ABSTRACT

Bilitranslocase is a plasma membrane carrier firstly identified on the sinusoidal (vascular) domain of liver cells and later on also in the gastric epithelium. It transports diverse organic anions, such as bilirubin, some phthaleins and many dietary anthocyanins, suggesting that it could play a role both in the absorption of flavonoids from dietary sources and in their hepatic metabolism. This work was aimed at characterising the interaction of bilitranslocase with flavonols, a flavonoid sub-class. The results obtained show that, contrary to anthocyanins, flavonol glycosides do not interact with the carrier, whereas just some of the corresponding aglycones act as relatively poor ligands to bilitranslocase. These data point to a clear-cut discrimination between anthocyanins and flavonols occurring at the level of the bilitranslocase transport site. A quantitative structure–activity relationship based on counter propagation artificial neural network modelling was undertaken in order to shed light on the nature of flavonoid interaction with bilitranslocase. It was found that binding relies on the ability to establish hydrogen bonds, ruling out the involvement of charge interactions. This requisite might be at the basis of the discrimination between anthocyanins and flavonols by bilitranslocase and could lie behind some aspects of the distinct pharmacokinetic properties of anthocyanins and flavonols in mammals.



## 1. Introduction

Flavonoids are heterocyclic, polyphenolic compounds featured by a common basic structure consisting of two aromatic rings (A and B), bound to an oxygenated heterocycle (ring C) (Fig. 1).

The chemical repertoire of flavonoids is large, due to different patterns of hydroxylation, methoxylation and

* *Corresponding author*. Tel.: +39 0405583681.
** *Corresponding author*.
E-mail addresses: spassamonti@units.it (S. Passamonti), marjana.novic@ki.si (M. Novič).
[1] Present address: Department of Physiology and Pathology, University of Trieste, 34127 Trieste, Italy.
*Abbreviations:* *CP-ANN, counterpropagation artificial neural network; BSP, bromosulfophthalein*
0006-2952/$ – see front matter © 2006 Elsevier Inc. All rights reserved.
doi:10.1016/j.bcp.2006.09.024

glycosylation of their common structure [1]. They are plant secondary metabolites occurring at relatively high amounts in several kinds of fruits, grains and vegetables harvested for human consumption [2]. The prevalence of such food in the human diet has recently been associated with significant reductions of the risk factors in significant chronic human pathologies, such as diabetes, cancer, neuro-degenerative and cardiovascular diseases [3–5].

At the cellular level, flavonoids have been found to exert a variety of biological effects [6], presumably mediated by specific interaction with molecular targets. Indeed flavonoids have been shown to interact with biological macromolecules, such as nucleic acids [7–9], polysaccharides [10,11] and proteins [12–15].

The critical step determining the ability of any compound to reach an intracellular target is its translocation through the cell plasma membrane, for which the activity of specific transport proteins is mandatory in the case of hydrophilic and sterically complex compounds [16]. One among the carriers possibly involved in flavonoid membrane transport is bilitranslocase (T.C. 2.A.65.1.1, [17]) a membrane transporter firstly identified in the liver [18], where it is expressed on the sinusoidal domain of the plasma membrane. At this level, its physiological function is to mediate the facilitated diffusion of organic anions from the blood into the liver, thus playing a role in the hepatic detoxification pathway(s) of endo- and xenobiotics.

Its established substrates are bilirubin [19,20] and nicotinic acid [19] with dissociation constants ($K_d$) of 2 and 11 nM, respectively, sulfobromophtalein ($K_d$ = 5 μM) [21,22] and anthocyanins ($K_d$ = 1.5–22 μM) [23].

The interaction mechanism of bilitranslocase binders has not yet been established. The problem is difficult to approach, because the secondary structure of bilitranslocase is not known. The investigation needs to be focused on the structural properties of the ligands in order to infer the mechanism(s) of their interaction with the transporter.

Thus, to better understand the interaction between flavonoids and the carrier, some additional compounds, 21 flavonols, were experimentally tested as inhibitors of bilitranslocase transport activity.

Furthermore, we studied the nature of the interactions between bilitranslocase and flavonoid ligands (both anthocyanins and flavonols) by counter propagation neural network (CP-ANN), one of the computational approaches already validated as a proper tool in the investigation of ligand activity [24]. We have used this approach first to classify the tested molecules into three classes, according to their effect on bilitranslocase transport activity: (i) competitive inhibitors (C), (ii) non-competitive inhibitors (N), (iii) inactive molecules (I); in addition, the inhibition constant values ($K_i$) of competitive inhibitors could be predicted. A special attention was dedicated to the examination of the kind of molecular descriptors needed to create the model. The results of this work show that, contrary to dietary anthocyanins, most of dietary flavonols do not interact with bilitranslocase, whereas, some flavonol aglycones act as poor ligands of that carrier. The quantitative analysis of the structure–activity relationship led to the identification of parts of ligands potentially involved in the binding to bilitranslocase, along with a reliable hypothesis on the kind(s) of interaction between the ligand and the target.

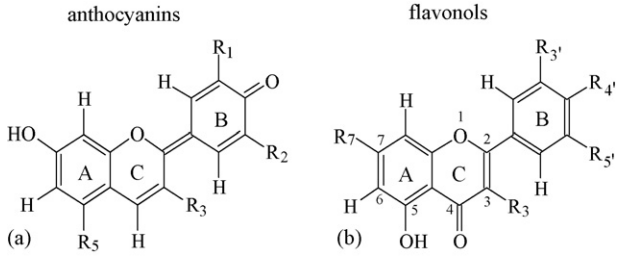


**Fig. 1 – Chemical structures of anthocyanins (a) and flavonols (b). The substitutions occur at positions denoted by *R* (see Table 2).**

## 2. Materials methods and models

### 2.1. *Flavonoids*

Compounds were purchased from the following commercial sources: ID 23 from Carl Roth GmbH + Co. KG (Karlsruhe, Germany), ID 24–28 and 38–43 from Extrasynthèse (Genay, France), ID 30–31 from Polyphenols Laboratories AS (Sandnes, Norway), ID 32 and 36–37 from Indofine Chemical Company Inc. (Hillsborough, NJ, USA), ID 33–35 from Fluka (Buchs, Switzerland). All other reagents were of the highest purity grade commercially available.

### 2.2. *Bilitranslocase transport activity assay*

Bilitranslocase transport activity was assayed spectrophotometrically in rat liver plasma membrane vesicles as described in detail in previous papers [22,23,25]. The assay employs the pH-indicator dye bromosulfophthalein (BSP) as the transport substrate, dissolved in a $K^+$-phosphate buffered transport medium. The concentration of BSP in the medium is recorded in real time by dual-wavelength spectrophotometry at λ = 580–514 nm. Following the addition of plasma membrane vesicles to the assay medium, BSP is allowed to attain its electrochemical equilibrium between the extra- and the intravesicular compartment. Then, a further entry of dye into vesicles is triggered by the $K^+$ diffusion potential generated by the addition of valinomycin to the assay medium. The initial rate of such BSP uptake is a specific measure of bilitranslocase transport activity [22,26]. In the assay, the potential is inverted by design to just boost BSP uptake into vesicles, and thus enhance the sensitivity of the method, and is the sole driving force of BSP uptake. In vivo, the negative membrane potential opposes the uptake of the anion BSP from the blood into the liver. Nevertheless, both glutathionylation of BSP and the active pumping of glutathionyl-BSP into the bile build up an ample chemical potential that outbalances the electrical one. For transport inhibition tests, 2–6 μl of flavonoids dissolved in dimethylsulfoxide (0.1–0.3%, vol:vol in the assay) at concentrations ranging 20–70 mM were added to the medium 5 s before the addition of vesicles, just as previously done in the screening of anthocyanins [23]. The interference of inhibitors with the optical signal was systematically assessed in appropriate control experiments. DMSO had no effect in the assay, within the chosen experimental conditions.

### 2.3. Theoretical section

#### 2.3.1. Counterpropagation artificial neural network

A detailed description of counterpropagation artificial neural network (CP-ANN) architecture and learning strategy have been described in several articles and textbooks [27–30].

Basically, the CP-ANN modelling is based on a two-step learning procedure, unsupervised in the first step, while supervised in the second one; both steps are completely independent, but have to follow each other in the iterative process of learning. As shown in Fig. 2, the architecture of CP-ANN is made of two layers of neurons represented as vectors of weights arranged in a two-dimensional rectangular matrix. The first layer of neurons, arranged in a two-dimensional plane, is named input or Kohonen layer and imitates with its structure and learning strategy the structure and function of the brain. The Kohonen layer has a well-defined neuron topology with a well-defined neighborhood structure. The number of neurons is related to the number of objects.

The supervised learning procedure (which is employed to train the artificial neural network) is determined by the input–output pairs $\{X_s, T_s\}$ of our data set. Descriptors ($X_s$) are used to mathematically characterise the molecular structure of objects (the compounds tested in our study) and will be described in the next section. The biological properties of the objects (active or inactive) are the targets $T_s$. During training each object, i.e. molecular structure $X$, triggers one of the neurons in the input layer. After a stepwise correction of weights, similar objects are placed close to each other, resulting in the formation of clusters that can be observed in the top-map of the CP-ANN. Learning in the output layer is different, because in each iteration the position of the triggered neuron is simply projected onto the output layer (vector *Out*, in Fig. 2 denoted with *y*).

In applying CP-ANN to the classification of flavonoid molecules, the corresponding target $T_s$ is a three-component binary vector indicating one out of three possible classes of bilitranslocase substrates (inactive, competitive and non-competitive inhibitors), while in the predictive model the target is the inhibition constant $K_I$. The training of the network means adjusting the neuron weights in such a way that the network would respond with the address of the most similar neuron for each object $X_s$ from the training set and with the output $Out_s$ most similar to the target $T_s$.

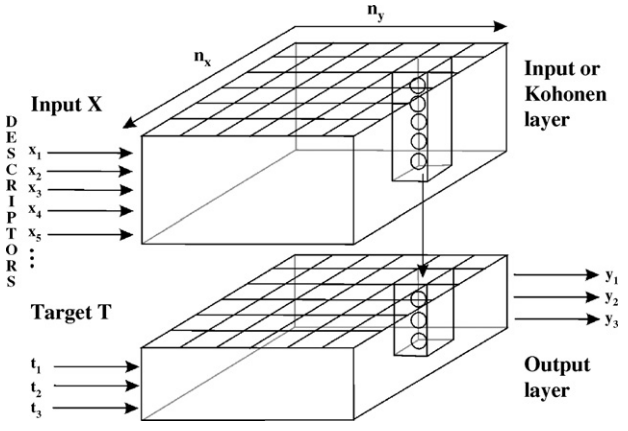


**Fig. 2 – The scheme of counterpropagation artificial neural network (CP-ANN).**

The training is an iterative procedure involving both feeding of all input–output pairs +d, to the network and correcting the weights of the neurons according to the differences between targets and current outputs ($T_s$–$Out_s$).

The unsupervised element in the CP-ANN learning procedure is the mapping of the molecule vectors into the Kohonen layer of the CP-ANN, which is based solely on the descriptors. Here descriptors play an important role, therefore they need to be carefully chosen (see next section) in order to obtain the best distribution and potential clustering of molecules within the top-map also called Kohonen map. For this step no knowledge about the target vector (activity class or $K_I$ value) is needed. Once the position (central neuron *c*) of the input vector is defined, the weights of the input and output layers of the CP-ANN are corrected accordingly. As a result, the trained network provides some information on the data set. Visual inspection of the top-map gives us information upon clusters as structural similarity relationships between objects. Descriptors, selected later on by genetic algorithm, will provide the knowledge about molecular features, which make the selected molecule, for instance, a good competitive inhibitor. Based on such a study we will be able to draw some hypothesis on the possible nature of the ligand–target interaction.

The trained network can be also used for prediction purposes. The predictions about a new object (from the set of testing molecules, which were not included in the training set) run in two steps. First it is situated in the Kohonen layer on the neuron with the most similar weights. This position is then projected onto the output layer, which provides the output value of $K_I$ or the class of substrate.

For CP-ANN modelling and genetic algorithm (see below) we used software developed in the laboratory of chemometrics at National Institute of Chemistry in Ljubljana [31]. The computational parameters of the neural network construction that can influence the results and should be tested and optimised are: number of training epochs (epochs), dimension of network ($n_x$, $n_y$), maximal correction factor ($a_{max}$), minimal correction factor ($a_{min}$).

#### 2.3.2. Structural descriptors and data set

The experimental data for the molecules listed in Table 2 were obtained by studying in vitro bilitranslocase transport activity as described above. The experimental data for anthocyanins were already published [23], while those for flavonols have been reported in this paper for the first time. The models for 22 anthocyanins and 21 flavonols were built up and the structural optimisation for each was performed. The semiempirical AM1 method within MOPAC packages [32] was used to obtain the equilibrated structures.

Next, the CODESSA program [33] was used to calculate the descriptors on the basis of optimised geometrical parameters. The set of descriptors are split into five categories: (i) constitutional descriptors, depending on the number and type of atoms, bonds, and functional groups; (ii) geometrical descriptors, which give molecular surface area, projections, and gravitational indices; (iii) topological descriptors, which are molecular connectivity indices, related to the degree of

branching in the compounds; (iv) electrostatic descriptors, such as partial atomic charges or hydrogen bonding attitudes of the molecules; (v) quantum-chemical descriptors, i.e. total energy of molecule, the energies of the lowest unoccupied and highest occupied orbitals, ionization potential, etc. All descriptors were normalised, maintaining the original distribution, by a range scaling procedure following the equation below:

$$x_{\text{norm}} = \frac{x_i - x}{s(x)}$$

where $x_{\text{norm}}$ is the normalised value of the descriptor $x_i$, $x$ the average value and $s$ is a standard deviation, calculated as follows:

$$s(x) = \sqrt{\frac{\sum (x_i - x)^2}{n-1}}$$

where $n$ is the number of molecules.

The crucial point of the chemometric method is to obtain a proper set of descriptors, which very often means a reduction in the number of the originally calculated descriptors. We got 353 descriptors for each molecule as CODESSA output.

The selection of variables was done for two independent purposes. First we wanted to classify the molecules according to their effect on bilitranslocase transport activity (inactive, competitive and non-competitive). We calculated the average of the absolute deviation and removed all descriptors with values smaller than 0.8. In this way we eliminated the non-discriminative variables similar for all molecules that could not help distinguishing them. The models were tested with the leave-one-out method [34]. The correlation coefficient of leave-one-out test ($R_{cv}$) was used as a criterion to estimate the quality of the classification models. In such a way we ended up with 207 descriptors.

Second, we wanted to predict the $K_I$ value of competitive inhibitors. For this purpose we used only 18 molecules from the data set, those that show the competitive inhibition of bilitranslocase. With these molecules we started the selection procedure once again with the whole set of descriptors. The initial selection was done using the transposed data matrix, in which one row is equal to an object representing one descriptor; it contains the values of one particular descriptor for all compounds. The dimension of the input vectors is now equal to the number of molecules in the data set. After inputting the transposed data matrix into the input layer of CP-ANN, we obtained the Kohonen map of descriptors. Some of them either occupied the same neuron or formed clusters. The descriptors, which occupied one single neuron were selected as specific and chosen to be submitted to the next selection method. In the next step we applied the genetic algorithm (GA) [31]. Such an algorithm is used in a number of problems, where either optimal values of a set of parameters or an optimal reduced set of parameters, resulting from a combination of original parameters, is sought. The origin of its name comes from its resemblance with the biological process: the GA consists of three basic processes mimicking Darwinian evolution: crossover, mutation and survival of the fittest. In the crossover step, new chromosomes are generated by mixing fractions of old ones, the so-called parents chromosomes. A mutation is introduced to randomly change individual bits of the chromosome. In the last step the survivors are chosen for the next generation, i.e. cycle of the GA. The survivors are the chromosomes having the best criterion value determined by the fitness function. This last step should yield the lowest possible number of descriptors, thus yielding a satisfactory prediction for $K_I$ for each individual inhibitor in the data set. The length of the chromosome, i.e. the number of genes or bits, is determined by the number of input parameters. Once again the leave-one-out cross-validation method for the training set data was used for verifying the models with different numbers of descriptors. The best results were obtained for the set of 155 variables and these results are presented in the following paragraph.

## 3. Results

### 3.1. *The effect of various flavonols on the transport activity of bilitranslocase in rat liver plasma membrane vesicles*

The inhibition constants of anthocyanins were already reported by Passamonti et al. [23], while those for the flavonols were obtained in this study. Out of 20 compounds tested, only three flavonols acted as inhibitors of electrogenic BSP uptake in rat liver plasma membrane vesicles, yielding the kinetic parameters of electrogenic BSP uptake listed in Table 1. The $K_I$ values of all compounds are given in Table 2.

### 3.2. *Classification model*

The set of 40 molecules was studied for the classification purpose. In this study, the model adaptive parameters are: number of training epochs, dimension of network ($n_x$, $n_y$) and maximal correction factor. We divided the molecules into the training and test sets on the basis of clusters formed on the Kohonen map. We took care to include into the test set all representatives of groups of structurally similar molecules. The CP-ANN was trained with the molecules of the training set with the following network parameters: $n_x = n_y = 6$, $a_{\max} = 0.3$, $a_{\min} = 0.01$, epochs = 200. The triangular correction function and non-toroidal condition were used for all CP-ANNs in this study.

The training molecules were well separated into clusters irrespective of their inhibition potency. The response surface with the predicted classes of molecules was originated from the supervised part of the CP-ANN training procedure. The testing set of molecules (ID 1, 6, 14, 17, 34, 40, 43; see Table 2) served for an evaluation of the classification model. All molecules were correctly classified, so we went one step further and tested our classification CP-ANN model with three other molecules, which had not been tested experimentally (ID 20, 21, 29; see Table 2). Two of them were classified as competitive inhibitors and one as an inactive molecule. The Kohonen map is illustrated in Fig. 3. After a detailed study of structures and descriptors of the compounds not experimentally tested and in the view of their similarity to experimentally tested molecules, we concluded that the classification was correct.

**Table 1 – Michaelis–Menten parameters of electrogenic bromosulphophthalein (BSP) uptake in rat liver plasma membrane vesicles in the presence of galangin (ID 23), kaempferol (ID 24) and quercetin (ID 25)**

| | $V_{max}$ (μmol min$^{-1}$ mg$^{-1}$ ± S.E.M.) | $K_M$ (μM ± S.E.M.) | Non-competitive $K_I$ (μM) | Competitive $K_I$ (μM) |
|---|---|---|---|---|
| ID 23 (μM) | | | | |
| 0 | 18.42 ± 0.23 | 5.22 ± 0.25 | – | – |
| 34 | 11.87 ± 0.04 | 5.31 ± 0.07 | 61.62 | – |
| 68 | 7.76 ± 0.18 | 5.42 ± 0.48 | 59.51 | – |
| | | | Mean ± S.E. 60.56 ± 1.05 | – |
| ID 24 (μM) | | | | |
| 0 | 16.62 ± 0.34 | 5.25 ± 0.41 | – | – |
| 23.6 | 12.21 ± 0.15 | 6.14 ± 0.30 | 65.34 | 140.00 |
| 44.25 | 10.01 ± 0.30 | 7.06 ± 0.71 | 67.01 | 128.28 |
| 59 | 7.94 ± 0.39 | 7.54 ± 1.11 | 53.94 | 135.38 |
| 37 | 10.84 ± 0.27 | 6.83 ± 0.59 | 69.20 | 122.77 |
| | | | Mean ± S.E. 63.9 ± 3.4 | Mean ± S.E. 131.6 ± 3.8 |
| ID 25 (μM) | | | | |
| 0 | 16.62 ± 0.34 | 5.25 ± 0.41 | – | – |
| 20 | 13.41 ± 0.24 | 9.46 ± 0.49 | 83.55 | 24.94 |
| 40 | 10.84 ± 0.74 | 14.62 ± 2.39 | 75.02 | 22.41 |
| 60 | 9.45 ± 0.94 | 24.16 ± 4.7 | 79.08 | 16.65 |
| 80 | 8.35 ± 0.91 | 25.79 ± 5.34 | 80.77 | 20.45 |
| | | | Mean ± S.E. 79.61 ± 1.79 | Mean ± S.E. 21.11 ± 1.75 |

The most problematic group for classification contained the non-competitive inhibitors. The data were available for only four molecules, i.e. ID 18, 19, 23, and 24. Molecule no. 25 (quercetin) was treated as competitive because of higher competitive than non-competitive $K_I$ (see Table 2). We even had to remove one of the non-competitive molecules (ID 18) from the training set, because it caused a conflicting situation with corresponding descriptors too similar to be distinguished from other competitive molecules. The general problem of the investigated molecules is that slight changes in the structure cause big changes in the activity. This was particularly evident with compounds ID 17 (Cyanidin 3-O-α-L-arabinopyranoside, competitive inhibitor) and ID 18 (Cyanidin 3-O-β-D-galactopyranoside, non-competitive inhibitor). In the final classification model only three non-competitive inhibitors were included (ID 19, 23, 24). A set of three compounds is obviously not enough for extracting the proper statistical evaluation of the predictions obtained by an experience-based model as CP-ANN is. We can

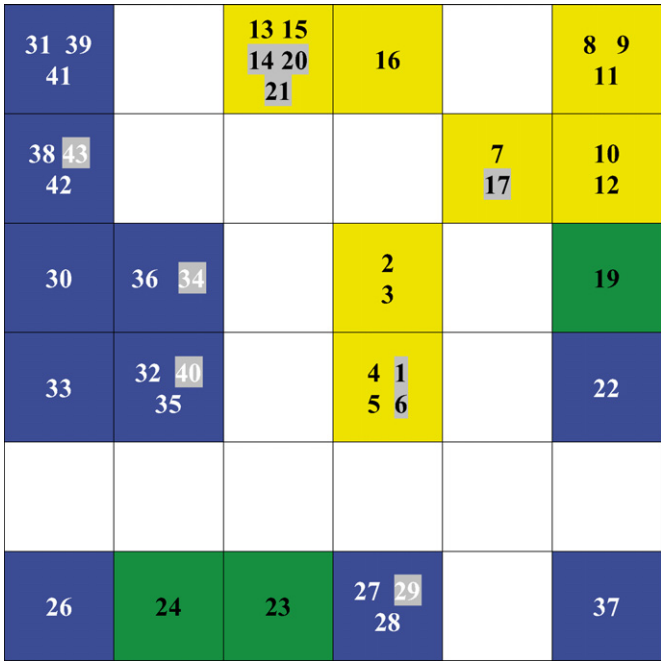


**Fig. 3 – The Kohonen map (top-map of the classification CP-ANN model, 6 × 6 neurons). The neurons occupied by the competitive, non-competitive or inactive ligands are colored yellow/dark grey, green/black or blue/light grey, respectively. The compounds are denoted by their ID numbers; the test compounds are highlighted to be distinguished from the training compounds.**

**Table 2 – Antocyanin and flavonol derivatives with experimental data on inhibition constants ($K_I$) of bilitranslocase transport activity; S.E.: standard error; R: substitutions at positions defined in Fig. 1**

| Compound | ID | $R_1$ | $R_2$ | $R_3$ | $R_5$ | $K_I$ | S.E. |
|---|---|---|---|---|---|---|---|
| Antocyanins | | | | | | | |
| Pelargonidin | 1 | H | H | OH | OH | 22.21[a] | 1.65 |
| Cyanidin | 2 | OH | H | OH | OH | 17.55[a] | 1.68 |
| Delfinidin | 3 | OH | OH | OH | OH | 5.27[a] | 0.38 |
| Peonidin | 4 | $OCH_3$ | H | OH | OH | 6.23[a] | 0.51 |
| Petunidin | 5 | $OCH_3$ | OH | OH | OH | 7.57[a] | 0.99 |
| Malvidin | 6 | $OCH_3$ | $OCH_3$ | OH | OH | 7.20[a] | 0.40 |
| Pelargonidin 3-O-β-D-glucopyranoside | 7 | H | H | β-D-Glucopyranosyl | OH | 2.79[a] | 0.18 |
| Cyanidin 3-O-β-D-glucopyranoside | 8 | OH | H | β-D-Glucopyranosyl | OH | 5.78[a] | 0.39 |
| Delfinidin 3-O-β-D-glucopyranoside | 9 | OH | OH | β-D-Glucopyranosyl | OH | 8.57[a] | 0.2 |
| Peonidin 3-O-β-D-glucopyranoside | 10 | $OCH_3$ | H | β-D-Glucopyranosyl | OH | 1.83[a] | 0.19 |
| Petunidin 3-O-β-D-glucopyranoside | 11 | $OCH_3$ | OH | β-D-Glucopyranosyl | OH | 4.03[a] | 0.19 |
| Malvidin 3-O-β-D-glucopyranoside | 12 | $OCH_3$ | $OCH_3$ | β-D-Glucopyranosyl | OH | 1.42[a] | 0.13 |
| Pelargonidin 3,5-di-O-β-D-glucopyranoside | 13 | H | H | β-D-Glucopyranosyl | β-D-Glucopyranosyl | 6.42[a] | 0.29 |
| Cyaniding 3,5-di-O-β-D-glucopyranoside | 14 | OH | H | β-D-Glucopyranosyl | β-D-Glucopyranosyl | 5.77[a] | 0.39 |
| Peonidin 3,5-di-O-β-D-glucopyranoside | 15 | $OCH_3$ | H | β-D-Glucopyranosyl | β-D-Glucopyranosyl | 6.81[a] | 0.77 |
| Malvidin 3,5-di-O-β-D-glucopyranoside | 16 | $OCH_3$ | $OCH_3$ | β-D-Glucopyranosyl | β-D-Glucopyranosyl | 6.36[a] | 0.45 |
| Cyanidin 3-O-α-L-arabinopyranoside | 17 | OH | H | α-L-Arabinopyranosyl | OH | 9.16[a] | 0.99 |
| Cyanidin 3-O-β-D-galactopyranoside | 18 | OH | H | β-D-Galactopyranosyl | OH | 35.22[b] | 0.58 |
| Malvidin 3-O-(6-O-acetoyl)-β-D-glucopyranoside | 19 | $OCH_3$ | $OCH_3$ | (6-O-Acetoyl)-β-D-glucopyranosyl | OH | 58.33[b] | 0.09 |
| Delfinidin 3,5-di-O-β-D-glucopyranoside | 20 | OH | OH | β-D-Glucopyranosyl | β-D-Glucopyranosyl | Not tested | – |
| Petunidin 3,5-di-O-β-D-glucopyranoside | 21 | $OCH_3$ | OH | β-D-Glucopyranosyl | β-D-Glucopyranosyl | Not tested | – |
| Malvidin 3-O-(6-O-*p*-coumaroyl)-β-D-glucopyranoside | 22 | $OCH_3$ | $OCH_3$ | (6-O-*p*-Coumaroyl)-β-D-glucopyranosyl | OH | I | I |

| Compound | ID | $R_3$ | $R_{3'}$ | $R_{4'}$ | $R_{5'}$ | $R_7$ | $K_I$ | S.E. |
|---|---|---|---|---|---|---|---|---|
| Flavonols | | | | | | | | |
| Galangin | 23 | OH | H | H | H | OH | 60.60[b] | 1.00 |
| Kaempferol | 24 | OH | H | OH | H | OH | 131.6[a], 63.90[b] | 3.80, 3.40 |
| Quercetin | 25 | OH | OH | OH | H | OH | 21.10[a], 79.60[b] | 1.70, 3.60 |
| Myricetin | 26 | OH | OH | OH | OH | OH | I | |
| Syringetin | 27 | OH | O–$CH_3$ | OH | O–$CH_3$ | OH | I | |
| Rhamnetin | 28 | OH | OH | OH | H | O–$CH_3$ | I | |
| Isorhamnetin | 29 | OH | O–$CH_3$ | OH | H | OH | Not tested | – |
| Quercetin 4′-glucopyranoside | 30 | OH | OH | Glu | H | OH | I | |
| Quercetin 3,4′-diglucopyranoside | 31 | Glu | OH | Glu | H | OH | I | |
| Quercetin 3-glucopyranoside | 32 | Glu | OH | OH | H | OH | I | |
| Quercetin 3-xyloside | 33 | Xyl | OH | OH | H | OH | I | |
| Quercetin 3-rhamnoside | 34 | Rham. | OH | OH | H | OH | I | |
| Quercetin 3-galactoside | 35 | Gal | OH | OH | H | OH | I | |
| Quercetin 3-O-gluco-pyranosyl-6″-acetate | 36 | Glu-Ac | OH | OH | H | OH | I | |
| Quercetin 3-O-sulfate | 37 | $SO_4$ | OH | OH | H | OH | I | |
| Isorhamnetin 3-glucoside | 38 | Glu | O–$CH_3$ | OH | H | OH | I | |
| Isorhamnetin 3-O-rutinoside | 39 | Rut | O–$CH_3$ | OH | H | OH | I | |
| Kaempferol-glucoside | 40 | Glu | H | OH | H | OH | I | |
| Kaempferol 3-O-rutinoside | 41 | Rut. | H | OH | H | OH | I | |
| Syringetin 3-galactoside | 42 | Gal | O–$CH_3$ | OH | O–$CH_3$ | OH | I | |
| Syringetin 3-glucoside | 43 | Glu | O–$CH_3$ | OH | O–$CH_3$ | OH | I | |

[a] Competitive inhibition.
[b] Non-competitive inhibition.

only say that the three non-competitive inhibitors, with the exception of ID 18 that was discarded, were separated from the other compounds (see Fig. 3, green/black squares). In the absence of test compounds, no prediction was possible.

### 3.3. *Model for prediction of $K_I$*

The prediction of $K_I$ is an essential step to validate the CP-ANN analysis of experimental data. To study the prediction of $K_I$ value, a set of 18 molecules was used, which experimentally show competitive activity. The molecules with ID numbers from 1 to 17 and quercetin (ID 25; see Table 2) belong to this set. Thanks to the 155 descriptors set and the computational parameters as follows: $n_x = n_y = 5$, $a_{max} = 0.3$, $a_{min} = 0.01$, epochs = 250, we obtained the Kohonen map reported in Fig. 4. The molecules are well clustered with respect to their $K_I$ values. However, perhaps even more significant, such clusters grouped molecules with various degree of glycosylation: the

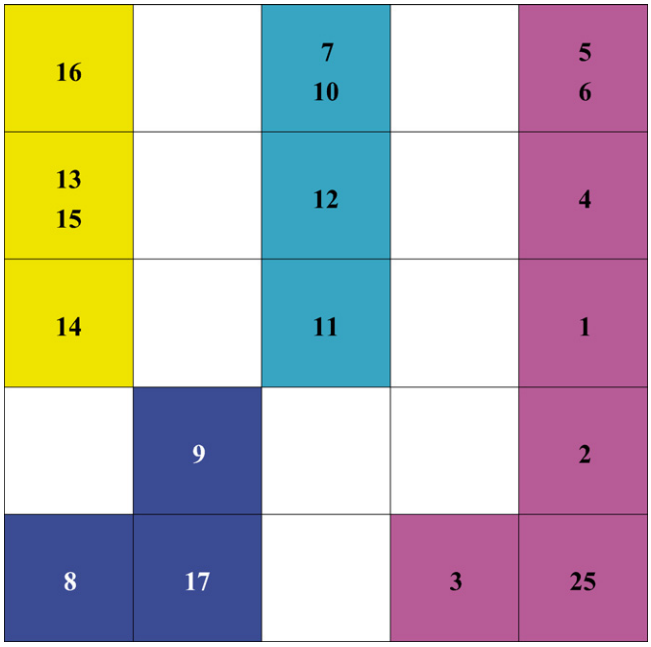


**Fig. 4 – The Kohonen map (top-map of the predictive CP-ANN model, 5 × 5 neurons). The ID numbers of 18 competitive inhibitors are shown as they appear in the trained network. The colors/intensity of grey indicate(s) structural similarity of groups of compounds: yellow/dark grey for diglucosides, pink/grey with texture for aglycones, grey and light grey/dark and light blue for monoglucosides with lower and higher affinity, respectively.**

yellow (dark grey) cluster gathers the di-glucosides, the pink (textured grey) cluster gathers the aglycones, and the blue (grey) cluster gathers the mono-glucosides with either higher (light blue (light grey)) or lower (dark blue (grey)) affinities for bilitranslocase.

The next modelling step was to split the molecules into the training and testing set. For the testing set we chose five molecules (ID 5, 7, 9, 16, 25). We trained the model until a suitable distribution of training molecules was obtained (Fig. 5a, black figures). The network parameters were the following: $n_x = n_y = 6$, $a_{max} = 0.35$, $a_{min} = 0.01$, epochs = 200. We tested the model with the molecules from the test set and, as a result, all the molecules (Fig. 5a, red (highlighted grey) figures) were placed in the correct clusters of trained molecules.

The predictions of the trained CP-ANN model are stored in the output (predictive) layer shown in Fig. 5b and c. From Fig. 5b it can be seen that we obtain 6 × 6 points of the $K_I$ response surface for 6 × 6 neurons in particular network architecture. The colour (grey scale) bar is given to associate the individual colour of the square with the $K_I$ value; the range 2–22 corresponds to the range of $K_I$ values of the training compounds. The prediction of a test compound is obtained by pinpointing a co-ordinate on the response surface. In Fig. 5c, a 3D view of the response surface with larger resolution (3 × 3 squares per neuron) is given. The colour (grey scale) bar is the same as in Fig. 5b.

The root mean squared error of prediction (RMSEP) of $K_I$ values is equal to 2.2. For a small dataset such as that investigated in the current study this error is expected. The $K_I$ values of the new molecules predicted by this model could be a good approximation of their actual values. We are especially satisfied with the results, because the tested molecules can be correctly placed in clusters of the training model. That result proves that the set of descriptors is properly chosen for prediction of $K_I$ value. Table 3 reports the experimental and predicted $K_I$ values.

### 3.4. *Structural descriptors influencing the binding of anthocyanins to bilitranslocase*

The detailed investigations of the 155 descriptors used to classify the compounds lead us to conclude that the ligand ability to act as hydrogen-bond donors and/or acceptors is very important for establishing an interaction with the host molecule. Descriptors directly defining the ability for creating this kind of bonds were indicated by an automated genetic-algorithm-based variable selection procedure. Only the selected descriptors enabled the CP-ANN training procedure to cluster the molecules according to their affinity to the target.

### 3.5. *Final validation of the CP-ANN model*

The final validation of the CP-ANN model was performed by testing the inhibition activity of BSP, which is an established substrate of bilitranslocase with the $K_I$ equal to 5.32 ± 0.63 μM [21,22]. The 3D structure was prepared in the same way as for all other molecules in the study (see Section 2.3.2). Once structural descriptors were obtained, only those selected in the model building and variable reduction procedure were accepted, i.e. 155 descriptors (the list of descriptors is available in supplementary materials). The predicted $K_I$ value was 4.03 (see Table 3), the difference between experimental and predicted value thus being 1.29. This error, though twice as

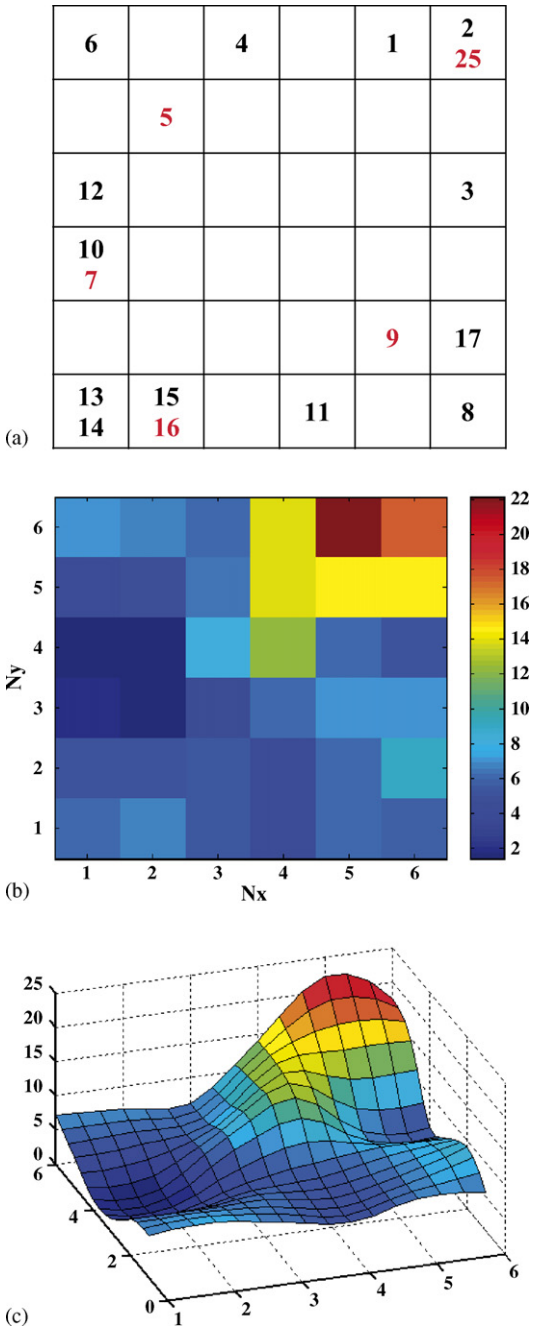


**Fig. 5 – The top-map with 6 × 6 neurons (a), the response surface (b), and 3D view of the response surface (c) of the final predictive CP-ANN model trained with 15 training compounds.**

large as the established experimentally (±0.63), was lower (nearly two-fold) than expected from the assessed model error (RMSEP = 2.2).

## 4. Discussion

The main result of this work consists in the identification of the nature of molecular interactions between the flavonoids and bilitranslocase. This enabled a structure-based classification of molecules according to their activity. Taking into account the structural features of the molecules belonging to a given cluster and focussing on the nature of molecular interactions between the carrier and the ligands, a system of deductions about the structural requirements for the activity of bilitranslocase ligands is proposed below.

**Table 3 – Experimental and predicted values (μM) of competitive inhibition constant for 18 compounds (13 training and five testing compounds, ID numbers given in Table 2) and for external test compound BSP (sulfobromophthalein)**

| ID | Experimental $K_I$ | Predicted $K_I$ |
|---|---|---|
| Training set | | |
| 1 | 22.21 | 22.16 |
| 2 | 17.55 | 17.59 |
| 3 | 5.27 | 5.27 |
| 4 | 6.23 | 6.23 |
| 6 | 7.20 | 7.20 |
| 8 | 5.78 | 5.81 |
| 10 | 1.83 | 1.83 |
| 11 | 4.03 | 4.03 |
| 12 | 1.42 | 1.42 |
| 13 | 6.42 | 6.09 |
| 14 | 5.77 | 6.09 |
| 15 | 6.81 | 6.80 |
| 17 | 9.16 | 9.13 |
| Testing set | | |
| 5 | 7.57 | 4.85 |
| 7 | 2.79 | 1.83 |
| 9 | 8.57 | 6.23 |
| 16 | 6.36 | 6.79 |
| 25 | 21.10 | 17.59 |
| External test compound | | |
| BSP | 5.32 | 4.03 |

### 4.1. *The structural basis of classification of molecules (C, N and I)*

To understand the structural basis for the partition of molecules in well separated clusters of inactive and active (competitive and non-competitive) molecules, a comparative analysis of structural and functional features of anthocyanins versus flavonols was particularly helpful.

#### 4.1.1. *Active versus inactive molecules: the importance of the 3D structure of the molecule*

The role played by the 3D structure of the ligands was noticed for the compounds 2 (cyanidin, an anthocyanidin) and 25 (quercetin, a flavonol) and their analogues 8 and 32, substituted with the sugar at position $R_3$ (2 → 8 and 25 → 32). Substitution on cyanidin (ID 2 → 8) made it a better inhibitor, since its $K_I$ decreased from 17.55 to 5.78 μM. On the contrary, substitution on quercetin (ID 25 → 32) made it an inactive molecule. We compared the optimised 3D structures of these molecules, which are shown in Fig. 6, and we noticed that they differ mostly in the orientation of the sugar moiety. The sugar in ID 8 lies in the same plane as the planar aromatic rings. In this way, the hydrogen atoms of the sugar OH

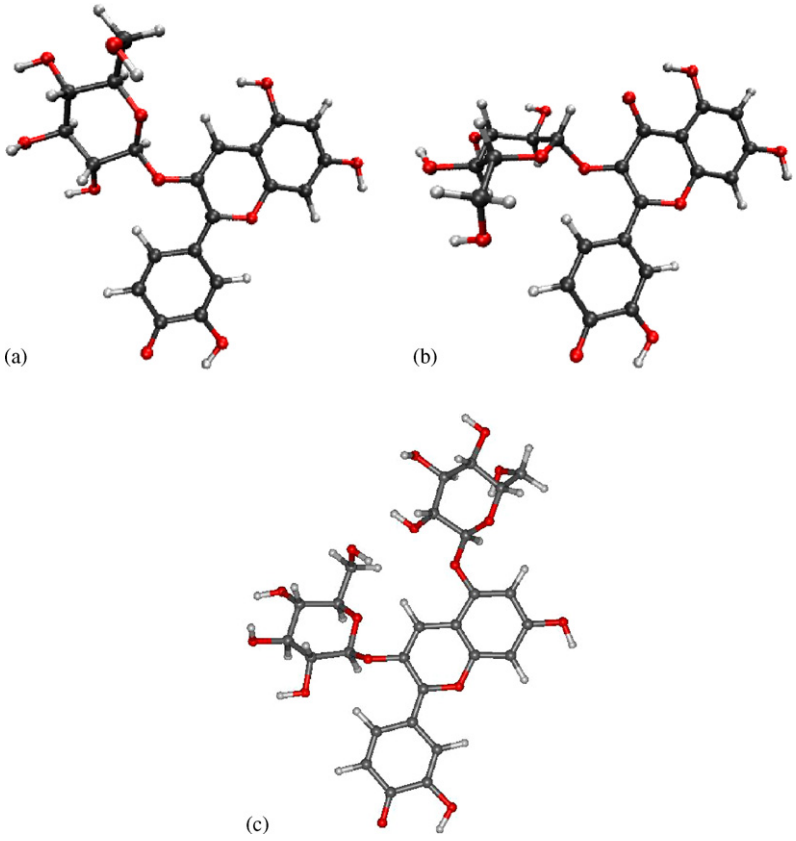


**Fig. 6 – 3D structures of (a) cyanidin 3-glucoside (ID = 8), (b) quercetin 3-glucoside (ID = 32) and (c) cyanidin 3,5-diglucoside (ID = 14).**

groups point to the same direction as the substitutes of B ring, ready to create hydrogen bond(s) with the target. On the contrary, the same sugar moiety bound to an equivalent position in quercetin is located perpendicularly to the planar condensed rings of the molecule. This position is forced by the presence of the oxygen atom in ring C. That may be a good reason for the molecule ID 32 to be inactive even in a protein environment—it simply does not fit the binding pocket of the host molecule. The energy needed to flip down the sugar moiety could be too high, especially if the carbonyl group of ring C acted as an H bond acceptor from the carrier active site. We looked at the structure of ID 14 (cyanidin 3,5-di-O-β-D-glucopyranoside), in order to evaluate the 3D structure of the two sugar substitutions. We found that both are almost co-planar with rings A and C. From these observations it can be deduced that the ligands of bilitranslocase, whether acting as competitive or non-competitive inhibitors, have to be planar. This conclusion is in agreement with the original experimental observation that the only phthalein tautomer transported by bilitranslocase is the planar, quinoidal one [25].

#### 4.1.2. *Competitive versus non-competitive inhibition by aglycones: the importance of hydroxylation of B ring*

As a step further, we tried to understand the structural basis underlying the property of bilitranslocase inhibitors to act either competitively or non-competitively. Some hints were provided by the behaviour of the three active flavonols (ID 23–25).

Galangin (ID 23) is the only aglycone displaying pure non-competitive activity. Unique among all flavonoid aglycones tested (both anthocyanins and flavonols), its ring B has no oxygen atom at position $R_{4'}$. We deduced that its interaction with the target must involve the condensed rings A and C, the only moieties suitable for H bond formation. By contrast, the introduction of an OH group in the 4′ position of the B ring of flavonols (as in ID 24 and 25) confers them the further property to interact at the level of the competitive site, like most of the anthocyanins (ID 1–19).

#### 4.1.3. *Pure competitive versus mixed-type inhibition: the possible role of tautomerism of ring B*

To understand the nature of mixed-type inhibition, typical of two flavonols (ID 24–25), we started from the evidence that the CP-ANN model clustered competitive molecules separately from non-competitive ones, reflecting two well distinct modes of interaction of the same molecule with the carrier. Given the importance of hydroxylation of the B ring in determining the type of inhibition (and its strength as well, as discussed below), we speculated that mixed-type inhibition is compatible with the binding of two alternative structures of ID 24–25 to the carrier, arising from pH-dependent phenolic-quinoidal tautomerism of the B ring (see Fig. 7). Given the fact that the $pK_a$ values of ID 24 and 25 are 8.1–8.2 and 7.0–7.03, respectively [35],

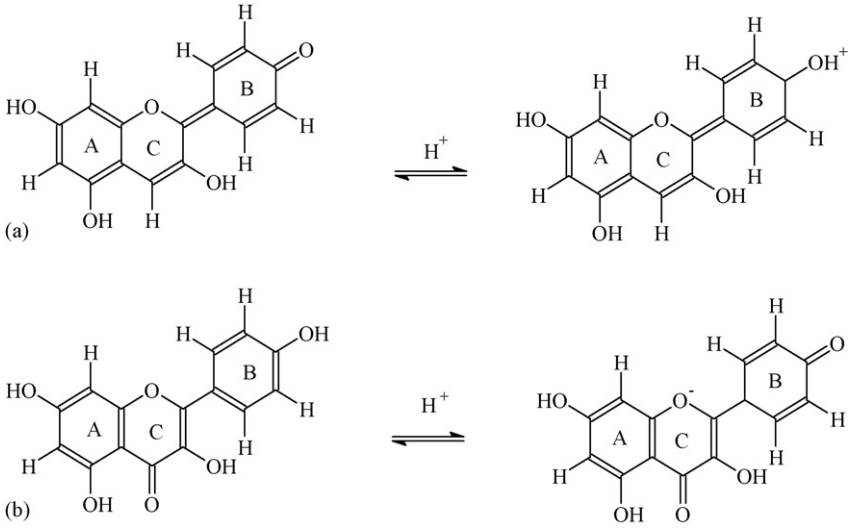


**Fig. 7 – pH-dependent tautomers of anthocianins (a) and flavonols (b).**

both tautomers of either ID 24 or 25 occur in the assay medium enough to generate mixed-type inhibition.

In the evaluation of this hypothesis, it should be observed that only flavonols have such dual activity, while anthocyanins are purely competitive inhibitors. Phenolic and quinoidal species of both classes of compounds occur in the assay medium. However, while the phenolic species of anthocyanins are cationic, those of flavonols are neutral.

The structural descriptors, selected by the genetic algorithm, that enabled both the classification and the prediction of the activity of competitive inhibitors (Figs. 4 and 5), referred to the capability of establishing H bonds. Interestingly, they did not include, and likely excluded, charge interactions with the target. If so, anthocyanin aglycones might be all pure competitive inhibitors simply because their phenolic species are cationic and, as such, could establish no interaction with the target. It should therefore be concluded that quinoidal tautomers are likely to be the species competitively interacting with the carrier. By contrast, both the phenolic and the quinoidal species of flavonols are neutral and both could therefore bind the carrier. However, while quinoidal species of flavonols would act as competitive inhibitors, in analogy with anthocyanins, phenolic species would act as non-competitive inhibitors, in analogy with galangin (ID 23) whose B ring cannot originate a quinoidal tautomer.

The concept that *para*-quinoidal species of flavonoids competitively interact with bilitranslocase is supported by the experimental evidence that the pH-indicator phthaleins are transported only as *para*-quinoidal species [25]; it is quite realistic that competitive inhibition of phthalein transport should be exerted by the structurally closest tautomer of flavonoids. Another point in favour of this concept is that only the *para*-quinoidal species of flavonols definitely set the B ring in the same plane of the rest of the molecule, a structural requirement for phthaleins to be transported and for glycosylated flavonoids to be active.

Yet, what would prevent phenolic species, freely rotating around C1, from binding to the competitive site? With respect to the formation of a network of H bonds, we have to deduce that the main, obvious difference between *para*-phenolic and *para*-quinoidal species is that the former are H bond donors, whereas, the latter are H bond acceptors. This would suggest that the decisive structural feature for a molecule to act as a competitive inhibitor of bilitranslocase transport activity is the availability of atoms acting as H-bond acceptors from corresponding H-bond donors of the active site of the carrier. Conversely, the H-bond formation by donating a hydrogen by a *para*-phenolic tautomer to the active site of the carrier might involve a configuration of the flavonol B ring compatible with non-competitive inhibition.

### 4.2. *The structural basis of the activity of competitive inhibitors*

The visual inspection of the Kohonen map shown in Fig. 4 highlights the relationship between the structure and the activity of investigated compounds. Clusters are formed according to the degree of glycosylation. The best competitive inhibitors are anthocyanin mono-glucosides, separated in two sub-classes grouping molecules with $K_I$ values $<4$ μM (ID 7, 10–12; light blue) and $>5.8$ μM (ID 8, 9, 17, dark blue), respectively. The di-glucosides form the next group, if ranged by affinity and the last are the aglycones, with the lowest affinity (in Fig. 4 shown as yellow and pink squares, respectively).

This map indicates that the carrier active site somehow ''reads'' the glycosylation state of anthocyanins, thus implying not only that it is a complex and multi-compliant structure, but also that it provides a polar environment for the interaction with polar moieties of the substrates.

#### 4.2.1. *Flavonoid aglycones: the importance of hydroxylation of the B ring*

Among competitive inhibitors, the least polar anthocyanidin (pelargonidin, ID 1) is the least active one ($K_I = 22.21$ μM). Similarly, the least polar flavonol (kaempferol, ID 24) has a

very poor competitive inhibition activity ($K_I$ = 131.6 μM). The presence of a second hydroxyl group on ring B, as in either cyanindin (ID 2, an anthocyanin) or in quercetin (ID 25, a flavonol), enhances the competitive inhibition of both compounds. While among anthocyanins the gain in activity is just above the statistical significance: $K_I = 22.2 \pm 1.65$ μM (ID 1) versus $K_I = 17.5 \pm 1.68$ μM (ID 2), the effect is marked among the flavonols, as the $K_I$ drops from $131.6 \pm 3.8$ μM (ID 24) to $21.1 \pm 1.7$ μM (ID 25). Interestingly, the difference in $K_I$ of either cyanidin (ID 2) or quercetin (ID 25) is not significant, suggesting that both compounds interact with the target through the moiety they have in common, i.e. the ring B. Thus, the number of H bonds established at the level of the B ring is indeed very important in shaping the strength of interaction of the aglycones. In more detail, the B ring interactions are based on the presence of two vicinal oxygen atoms, possibly acting as a couple of H bond acceptor (the *para*-quinoid carbonyl) and H bond donor (the $R_{3'}$ hydroxyl group). At the same time, the steric hindrance exerted by the carbonyl group of the C ring, a specific feature of the flavonols, appears to be successfully overcome if the B ring interactions prevail over the others.

#### 4.2.2. *Flavonoid aglycones: the importance of steric hindrance and charge distribution caused by the carbonyl group of the C ring*

The carbonyl group of ring C in flavonols appears to heavily influence the magnitudes of the competitive $K_I$ values. That was realised by comparing pelargonidin (ID 1 an anthocyanin) with kaempferol (ID 24, a flavonol). The anthocyanin is nearly six-fold more active than the flavonol (22.2 μM versus 131.6 μM). The flavonol appears to be sterically hindered by the carbonyl group of the C ring. It can be also considered that the carbonyl group on the C ring favours the establishment of intra-molecular H bonds with the OH groups in $R_3$ or in $R_5$ [35], thus possibly limiting the overall tendency of flavonols to interact with the carrier and therefore increasing their apparent competitive $K_I$.

In flavonols, the presence of a hydroxyl group in $R_{5'}$ (ID 26 versus ID 23, 24, 25) or, as predicted by the CP-ANN (Fig. 3), *O*-methylation of the B ring (ID 29 versus ID 25) results in the total loss of activity. In none of the anthocyanins were these all-or-none effects observed on activity (ID 3 versus ID 1, 2 and ID 4 versus ID 2). On the contrary, triple hydroxylation of the B ring of anthocyanins is better than double hydroxylation (ID 3 versus ID 2) and *O*-methylation is also well accepted, apparently because the anthocyanin aglycone can interact with the target also through the A ring, as previously proposed [23]. In flavonols, the functional groups introduced in the B ring, as in ID 26 and ID 29, appear to be equally effective in preventing their interaction with the carrier, presumably by steric hindrance. It results therefore that the carbonyl group of the C ring in flavonols acts as constraint for their ability to take different orientations at the level of the transport site(s) of the carrier. Thus, in interacting with the carrier, flavonols might be seen as rather stiff molecules, with a limited repertoire of interactions, whereas, anthocyanins appear to be more flexible and thus better at fitting the chemical environment of bilitranslocase active site.

#### 4.2.3. *Anthocyanidin mono- and di-glucosides*

The distinctive feature for clustering mono-glucosides in two groups according to their activity (Fig. 4, light and dark blue) is the OH group at position $R_1$ of the B ring, which occurs in the low-affinity molecules ($K_I > 5.8$ μM, ID 8, 9, 17) and is missing in the high-affinity ones($K_I < 4$ μM ID 7, 10–12). In the case of mono-glucosides, an increase in the polarity of B ring (see Table 2) lowers the affinity for the target (ID 7–9, 10–12). While this finding emphasises one more time the critical role of this moiety in the interaction with the carrier, it also reflects the existence of a specific binding pocket for the glycosyl moiety attached to C3, improving the binding affinity to such an extent that the interaction with the B ring is devalued. Furthermore, any changes in the sugar moiety result in the decrease of affinity to the target (e.g. ID 8 versus ID 17) or even in a change of the type of inhibition (e.g. ID 8 versus ID 18 and ID 19; Table 2). This may be an indication that the ligand does interact with the target at two sites, i.e. at one site through the sugar moiety and at the other through the B ring.

But in the case of diglucosides, changes at substituents of ring B do not influence the $K_I$ value so much. That can suggest that the diglucoside-target interactions occur either through both sugars or through ring A and its glucosyl moiety, as proposed earlier [23].

It appears therefore that the target has a structurally complex active site, providing specific, hydrogen bond-based interactions for a potentially wide spectrum of structurally unrelated ligands.

### 4.3. *A hypothesis for the structural basis of the activity of ID 18*

A glycosyl moiety in C3 improves the interaction of anthocyanins with the carrier, because an additional set of H bonds can be established. Cyanidin 3-*O*-β-D-galactopyranoside (ID 18) clustered with competitive inhibitors, without being one. This would indicate that ID 18 might indeed bind to the carrier at the same level as the other mono-glucosides, although with lower affinity ($K_I$ = 35.2 μM versus $K_I$ = 1.42–9.16 μM). This concept is in apparent conflict with the tenet that non-competitive inhibitors bind to a site that is close to, but does not coincide with an enzyme active site. However, binding of the galactosyl moiety to the sugar-specific pocket of the carrier might affect the conformation of the active site of the carrier, thus perturbing the kinetics of BSP transport. Two possibilities are equally applicable, i.e. ID 18 either induces an alternative, catalytically less efficient, conformational modification of the transport site or it causes a blockade of a conformational modification essential for transport catalysis.

## 5. Conclusions

It can be concluded that the requirement for a flavonoid molecule to interact with the target is the overall planarity. Then, to interact in a competitive way, and thus to be presumably transported, it has to have a *p*-quinoid group on the ring B, in order to be a hydrogen bond acceptor. If it has a *p*-hydroxyl group on the ring B, it is a non-competitive inhibitor. The OH group may therefore play a dual role, either as a proton donor, or, in the deprotonated form, as a strong hydrogen bond acceptor. It would remain a challenge to determine the $pK_a$ value of polyphenols at their binding site.

It cannot be stated yet that inhibitors of electrogenic BSP transport activity are indeed transported, unless they are tested directly as transport substrates. However, the dependence of the interaction of flavonoids with bilitranslocase on H bonds shows that those molecules interact without charge compensation, an essential requirement to be transported electrogenically. By an independent experimental approach, transport of malvidin 3-glucoside in liver cells has been shown to be mediated by bilitranslocase [36], suggesting that, at least for competitive inhibitors, this could be the case.

Finally, the data presented above might help understand some aspects of the distinct pharmacokinetics of anthocyanins and flavonols. Following oral ingestion, anthocyanins are rapidly absorbed in the form of glucosides [37] already from the upper gastro-intestinal tract [38], were bilitranslocase is expressed [39]. By contrast, with the notable exception of quercetin, orally ingested quercetin glycosides are not absorbed from the rat stomach [40] and are extensively metabolized in the gastro-intestinal tract prior to their absorption into the enterocyte and passage into blood [41]. This situation could result at least in part from the fact that bilitranslocase does not interact with flavonol glycosides, thus it cannot mediate their trans-membrane transport as such. Conversely, bilitranslocase could play a role in the intestinal uptake of some flavonol aglycones, released in the gut lumen by the action of glycosidases such as lactase phlorizin hydrolase [41]. This hypothesis is further supported by observations of quercetin uptake in Caco-2 cell cultures (Michela Terdoslavich and Sabina Passamonti, unpublished data).

## Acknowledgements

A. Karawajczyk was a recipient of a Marie Curie fellowship (Marie Curie Host Training Site no. HPMT-CT-2001-00240); Dr. Ganiyu Oboh was a Junior Associate of the International Centre for Theoretical Physics, Trieste, Italy. The financial supports by the Universities of Trieste and the Ministero dell'Istruzione, Università e Ricerca (PRIN projects 2004070118), Banca di Credito Cooperativo del Carso/Zadružna Kraska Banka and Slovenian Ministry of Higher Education, Science and Technology (P1-017) are acknowledged. The kind gift of a number of flavonols used in this study by Dr. Fulvio Mattivi (Istituto Agrario di San Michele all'Adige, Italy) and the critical reading of the manuscript by Dr. Roberto Cecotti (University of Trieste) are acknowledged.

## Appendix A. Supplementary data

Supplementary data associated with this article can be found, in the online version, at doi:10.1016/j.bcp.2006.09.024.

## REFERENCES

[1] Harborne JB, Baxter H. Handbook of natural flavonoids John Wiley & Sons; 1999.
[2] Manach C, Scalbert A, Morand C, Remesy C, Jimenez L. Polyphenols: food sources and bioavailability. Am J Clin Nutr 2004;79(5):727–47.
[3] Morris BJ. A forkhead in the road to longevity: the molecular basis of lifespan becomes clearer. J Hypertens 2005;23(7):1285–309.
[4] Luchsinger J, Mayeux R. Dietary factors and Alzheimer's disease. Lancet Neurol 2004;3(10):579–87.
[5] Vita JA. Polyphenols and cardiovascular disease: effects on endothelial and platelet function. Am J Clin Nutr 2005;81(1):292S–7S.
[6] Middleton Jr E, Kandaswami C, Theoharides TC. The effects of plant flavonoids on mammalian cells: implications for inflammation, heart disease, and cancer. Pharmacol Rev 2000;52(4):673–751.
[7] Rahman A, Fazal F, Greensill J, Ainley K, Parish JH, Hadi SM. Strand scission in DNA induced by dietary flavonoids: role of Cu(I) and oxygen free radicals and biological consequences of scission. Mol Cell Biochem 1992;111(1/2):3–9.
[8] Solimani R. The flavonols quercetin, rutin and morin in DNA solution: UV–vis dichroic (and mid-infrared) analysis explain the possible association between the biopolymer and a nucleophilic vegetable-dye. Biochim Biophys Acta 1997;1336(2):281–94.
[9] Kanakis CD, Tarantilis PA, Polissiou MG, Diamantoglou S, Tajmir-Riahi HA. DNA interaction with naturally occurring antioxidant flavonoids quercetin, kaempferol, and delphinidin. J Biomol Struct Dyn 2005;22(6):719–24.
[10] Zheng Y, Haworth IS, Zuo Z, Chow MS, Chow AH. Physicochemical and structural characterization of quercetin-beta-cyclodextrin complexes. J Pharm Sci 2005;94(5):1079–89.
[11] Calabro ML, Tommasini S, Donato P, Raneri D, Stancanelli R, Ficarra P, et al. Effects of alpha- and beta-cyclodextrin complexation on the physico-chemical properties and antioxidant activity of some 3-hydroxyflavones. J Pharm Biomed Anal 2004;35(2):365–77.
[12] Jacobs MN, Lewis DF. Steroid hormone receptors and dietary ligands: a selected review. Proc Nutr Soc 2002;61(1):105–22.
[13] Di Pietro A, Conseil G, Perez-Victoria JM, Dayan G, Baubichon-Cortay H, Trompier D, et al. Modulation by flavonoids of cell multidrug resistance mediated by P-glycoprotein and related ABC transporters. Cell Mol Life Sci 2002;59(2):307–22.
[14] Hollosy F, Keri G. Plant-derived protein tyrosine kinase inhibitors as anticancer agents. Curr Med Chem Anticancer Agents 2004;4(2):173–97.
[15] Williams RJ, Spencer JP, Rice-Evans C. Flavonoids: antioxidants or signalling molecules? Free Radic Biol Med 2004;36(7):838–49.
[16] Ito K, Suzuki H, Horie T, Sugiyama Y. Apical/basolateral surface expression of drug transporters and its role in vectorial drug transport. Pharm Res 2005;22(10): 1559–77.
[17] Saier Jr MH. A functional-phylogenetic classification system for transmembrane solute transporters. Microbiol Mol Biol Rev 2000;64(2):354–411.
[18] Sottocasa GL, Lunazzi GC, Tiribelli C. Isolation of bilitranslocase, the anion transporter from liver plasma membrane for bilirubin and other organic anions. Meth Enzymol 1989;174:50–7.
[19] Battiston L, Passamonti S, Macagno A, Sottocasa GL. The bilirubin-binding motif of bilitranslocase and its relation to conserved motifs in ancient biliproteins. Biochem Biophys Res Commun 1998;247(3):687–92.
[20] Passamonti S, Terdoslavich M, Margon A, Cocolo A, Medic N, Micali F, et al. Uptake of bilirubin into HepG2 cells

assayed by thermal lens spectroscopy. FEBS J 2005;272(21):5522–35.
[21] Sottocasa GL, Baldini G, Sandri G, Lunazzi G, Tiribelli C. Reconstitution in vitro of sulfobromophthalein transport by bilitranslocase. Biochim Biophys Acta 1982;685(2):123–8.
[22] Passamonti S, Battiston L, Sottocasa GL. Bilitranslocase can exist in two metastable forms with different affinities for the substrates—evidence from cysteine and arginine modification. Eur J Biochem 1998;253(1):84–90.
[23] Passamonti S, Vrhovsek U, Mattivi F. The interaction of anthocyanins with bilitranslocase. Biochem Biophys Res Commun 2002;296(3):631–6.
[24] Novic M, Vracko M. Comparison of spectrum-like representation of 3D chemical structure with other representations when used for modelling biological activity. Chemomet Intell Lab Syst 2001;59(1/2):33–44.
[25] Passamonti S, Sottocasa GL. The quinoid structure is the molecular requirement for recognition of phthaleins by the organic anion carrier at the sinusoidal plasma membrane level in the liver. Biochim Biophys Acta 1988;943(2):119–25.
[26] Miccio M, Baldini G, Basso V, Gazzin B, Lunazzi GC, Tiribelli C, et al. Bilitranslocase is the protein responsible for the electrogenic movement of sulfobromophthalein in plasma membrane vesicles from rat liver: immunochemical evidence using mono- and poly-clonal antibodies. Biochim Biophys Acta 1989;981(1):115–20.
[27] Zupan J, Novic M, Ruisanchez I. Kohonen and counterpropagation artificial neural networks in analytical chemistry. Chemomet Intell Lab Syst 1997;38(1):1–23.
[28] Leardi Re. Nature-inspired methods in chemometrics: genetic algorithms and artificial neural networks (Data Handling in Science & Technology) Elsevier; 2003.
[29] Friedman JH, Cherkassky V. From statistics to neural networks: theory and pattern recognition applications Springer–Verlag; 1994.
[30] Dayhof J. Neural network architectures, an introduction New York: Van Nostrand Reinhold; 1990.
[31] Zupan J, Novic M. Optimisation of structure representation for QSAR studies. Analyt Chim Acta 1999;388(3):243–50.
[32] Dewar MJS, Zoebisch EG, Healy EF, Stewart JJP. The development and use of quantum-mechanical molecular-models. 76. AM1—a new general-purpose quantum-mechanical molecular-model. J Am Chem Soc 1985;107:3902–9.
[33] Katritzky AR, Lobanov VS, Karelson M. CODESSA 2.0, comprehensive descriptors for structural and statistical analysis, Copyright © 1994–1996 USA: University of Florida; 1994.
[34] Cherkassky V, Wechsler H, Friedman JH. From statistics to neural networks: theory and pattern recognition applications. NATO Advanced Study Institute 'From statistics to neural networks, theory and pattern recognition applications'. Les Arcs, Bourg Saint Maurice, France: Springer–Verlag Berlin and Heidelberg GmbH & Co. K, 1993. p. 406.
[35] Lemanska K, Szymusiak H, Tyrakowska B, Zielinski R, Soffers AE, Rietjens IM. The influence of pH on antioxidant properties and the mechanism of antioxidant action of hydroxyflavones. Free Radic Biol Med 2001;31(7):869–81.
[36] Passamonti S, Vanzo A, Vrhovsek U, Terdoslavich M, Cocolo A, Decorti G, et al. Hepatic uptake of grape anthocyanins and the role of bilitranslocase. Food Res Int 2005;38:953–60.
[37] Manach C, Williamson G, Morand C, Scalbert A, Remesy C. Bioavailability and bioefficacy of polyphenols in humans. I. Review of 97 bioavailability studies. Am J Clin Nutr 2005;81(1):230S–42S.
[38] Passamonti S, Vrhovsek U, Vanzo A, Mattivi F. The stomach as a site for anthocyanins absorption from food. FEBS Lett 2003;544(1–3):210–3.
[39] Nicolin V, Grill V, Micali F, Narducci P, Passamonti S. Immunolocalisation of bilitranslocase in mucosecretory and parietal cells of the rat gastric mucosa. J Mol Histol 2005;36(1):45–50.
[40] Crespy V, Morand C, Besson C, Manach C, Demigne C, Remesy C. Quercetin, but not its glycosides, is absorbed from the rat stomach. J Agric Food Chem 2002;50(3):618–21.
[41] Day AJ, Gee JM, DuPont MS, Johnson IT, Williamson G. Absorption of quercetin-3-glucoside and quercetin-4′-glucoside in the rat small intestine: the role of lactase phlorizin hydrolase and the sodium-dependent glucose transporter. Biochem Pharmacol 2003;65(7):1199–206.